ORIENTAL JOURNAL OF CHEMISTRY
An International Open Free Access, Peer Reviewed Research Journal
www.orientjchem.org
Est. 1984
ISSN: 0970-020 X
CODEN: OJCHEG
2017, Vol. 33, No. (1):
Pg. 418-429

Correlation of Ionic Imprinting Cavity Sites on the Amino-Silica Hybrid Adsorbent with Adsorption Rate and Capacity of Cd^{2+} Ion in Solution

BUHANI*, DIAN HERASARI, SUHARSO and SURIPTO DWI YUWONO

Department of Chemistry, Faculty of Mathematic and Natural Sciences,
University of Lampung, Indonesia.
*Corresponding author E-mail: buhani_s@yahoo.co.id

http://dx.doi.org/10.13005/ojc/330149

(Received: January 06, 2017; Accepted: January 31, 2017)

ABSTRACT

In this research, it has been evaluated concentration effect of Cd^{2+} ion used as the Cd^{2+} ionic imprinted on synthesis of the Cd^{2+} ionic imprinted amino-silica hybrid (Cd(II)-IIP) adsorbent to adsorption rate and capacity of the target ion (Cd^{2+}) in solution. The results of the ionic imprinting (as active sites of Cd^{2+} ion) obtained were prepared from different concentrations of the Cd^{2+} ion producing the different ionic imprinted cavity fraction. The concentrations of Cd^{2+} ion used as the ionic imprinting were 0.05, 0.10, and 0.15 mol L^{-1} resulting the ionic imprinted cavity fraction for each 97.89 (Cd(II)-IIPa), 98.49 (Cd(II)-IIPb), and 95.82 % (Cd(II)-IIPc), respectively. From the adsorption data obtained, they show that initial concentration differences of the imprinted Cd^{2+} ion produce different adsorption models of the Cd^{2+} ion. The bigger the Cd^{2+} ionic imprinting fraction, the higher the adsorption rate (k_1) and capacity (q) of Cd^{2+} ion on the adsorbent.

Keywords: Imprinted ionic; Adsorption; Amino-silica hybrid; Adsorption active site.

INTRODUCTION

Increasing of heavy metal using in a life activity has given the negative impact as environmental pollution derived from an industrial processing or heavy metal using at an environment[1-3]. Cd is one of heavy metals much more used in industry such as; gold coating industry, battery, rubber, and pigment used in ink, paint, as well as plastic[4]. The Cd metal is also exist naturally and also found in food although in small amount adsorbed by intestines 5-8 %. Cd is not biodegradable and it can be accumulated in human or animal body for a long time. The long-term exposure is associated with a renal dysfunction, obstructive lung diseases such as lung cancer. Cd may also produce bone defects (osteomalacia and osteoporosis) in humans and animals[5].

In recent years, an adsorbent synthesis to bind heavy metals runs continuously to reduce theirs concentration and spreading in an environment especially in water[6-8]. Success of heavy metal adsorption process depends on the adsorbent types used. Selection of the adsorbents will determine selectivity parameters and adsorption capacity to heavy metals. Criteria of good adsorbent to be improved is not soluble in water and organic solvent, having big specific surface area, high adsorption capacity and selectivity to metals which will be separated, and reusability for continuous extraction[9,10].

Ability of the adsorbent to bind heavy metals is very affected by active site availability on adsorbent. Several researches were performed to increase a number of active sites through adsorbent modification with adding specific functional groups[11,12]. In addition, it was performed increasing of the adsorbent active site selectivity to target metal ion *via* an ionic imprinting technique[13-18].

The ionic imprinted material synthesis technique is a potential technique to produce a selective material to metal ions. In the ionic imprinting technique, adsorption selectivity of metal ions can be produced because existence of metal ions plays a role as a template and a monomer containing functional groups in a polymer synthesis. Releasing of metal ions as template from a polymer matrix will cause a formation of ionic imprinted cavities and an arrangement on the ionic imprinted material which will bind target ion selectively[19-21]. In addition, the ionic imprinted material is relatively cheap and it can be stored at room temperature for a long time.

Effect of the active sites from modification result with addition of functional groups and ionic imprinting process to improve selectivity on adsorbent in adsorbing metal ion (adsorbate) can be known through evaluation of kinetic parameter and adsorption isotherm of metal ion with adsorbent[22-24]. In this paper, it was studied the effect of the active sites as the amino-silica hybrid ionic imprinted fraction on adsorption rate and adsorption capacity of Cd(II) ion from solution because equilibrium provide fundamental physicochemical data for evaluating the applicability of sorption processes as unit operation[25]. Chemical equilibrium is described by isotherm equation expressing surface characteristic and adsorbent active site affinity at certain temperature and pH. The adsorbent containing different number and active site type will have a different adsorption characteristics.

The effect of ionic imprinted cavity fraction formed as the active sites on adsorption characteristic was studied with interacting the adsorbent containing different ionic imprinted (template) concentrations to Cd^{2+} ion in solution. The interaction was evaluated with a kinetic model and an adsorption isotherm to determine the adsorption rate, adsorption isotherm model, and adsorption capacity value. Besides that, in the solution effect of pH is very important because the existence of H^+ ions which is big enough will competitive with metal ions to place the active sites on adsorbent which will influence the ability of metal ion adsorbed [26]. In this paper also, it was studied the adsorption model of metal ions on the ionic imprinted material with H^+ ion concentration variety to the active sites availability to bind the Cd^{2+} ions from solution.

MATERIALS AND METHODS

Materials and equipments

Reagent used in this work consisted of 3-aminopropyl-trimetoxyslane (APS), from Aldrich, TEOS, $CdCl_2{\cdot}H_2O$, Na_2EDTA, CH_3COOH, ethanol, CH_3COONa, and filter paper Whatman 42 from E-Merck, as well as HCl and NaOH from Alba. Apparatus used besides standard glass, it was also used supporting and analysis apparatus. The supporting apparatus consists of analytical balance (Mettler AE 160), sieve (200 mesh), and oven (Fisher Scientific), magnetic stirrer, centrifuge (OSK 6474B Centrifuge), and pH meter (Orion 4 Star). Analysis instrumentation performed in this research consisted of an atomic adsorption spectrophotometer (AAS) (Perkin Elmer 3110) applied to calculate the metal concentration and IR spectrophotometer (Prestige 21 Shimadzu) used to analyze the functional groups. Identification of surface morphology and element composition were performed with using a SEM-EDX (JSM 6360 LA). Identification of the material surface area was applied by surface area analyzer (Quantachrome Nova 1200e).

Adsorbent Preparation

In Cd(II)-IIP synthesis, the synthesis used

APS compound, solution interacted was made into 2 parts consisting of A solution containing mixture of TEOS and water, 10 mL, filled into the plastic container and added HCl 1 M up to pH 2. Then, it was stirred by a magnetic stirrer for 30 min. Solution of B contains 5 mL of Cd^{2+} solutions in ethanol with each 0.05, 0.10, and 0.15 mol L^{-1} to produce adsorbents of Cd(II)-IIPa, Cd(II)-IIPb, and Cd(II)-IIPc, respectively. Then, it was added each with 1 mL of APS stirred until to be homogeneous. The solution A and B were mixed with stirring using a magnetic stirrer for 30 min. Gel formed was left for a night, it was rinsed with water/ethanol mixture 60/40 % continued with soaking for 24 h in Na_2EDTA 0.1 M and stirred for 30 minutes in HCl 0.5 M. Then, the material obtained was neutralized by water up to pH ≈ 7, dried in oven for 6 h at temperature of 60 °C, and grounded until size of 200 meshes. For non-ionic imprinted adsorbent (NIP) was prepared without the Cd^{2+} ion[27].

Batch adsorption experiments

Experiments were performed with interacting 50 mg of the adsorbent in a series of Erlenmeyer flasks containing Cd^{2+} ion solution with concentrations of 0.0–250.0 mg L^{-1}. The adsorption was carried out in a batch system using a stirrer at optimum pH of 6 for 2 h and at 27°C[27]. Then, the solution was centrifuged and the filtrate was taken to analyze the metal concentration left in the solution with AAS.

Influence of H^+ ion concentration was studied with interacting 50 mg of the adsorbent with Cd^{2+} ions for 24 h at the H^+ ion concentrations for each 0.5, 1.0, 1.5, 2.5, and 5.0 mmol L^{-1}. Then, the solution was also centrifuged and the filtrate was taken to calculate the metal concentration left in the solution with AAS.

The amount of Cd(II) ion adsorbed *q* (mg g^{-1}) by NIP and Cd(II)-IIP adsorbent was calculated using Equation 1:

$$q = \frac{v(c_i - c_f)}{m} \quad ...(1)$$

where c_i and c_f are initial and final concentration of the Cd^{2+} ion in solution, *v* is solution volume (L), and *m* is adsorbent mass (g).

To investigate the adsorption process optimization, it was performed correlation approach between the Cd^{2+} ion amount adsorbed experimentally with a batch method and the Cd^{2+} ion amount adsorbed estimatically *via* the adsorption isotherm equations using Langmuir, Freundlich, Dubinin-Radushkevich, and Temkin model. The isotherm model parameters were evaluated to determine the root mean squared error (*RMSE*) and Chi-square test (χ^2)[16,22] with these equations below:

$$RMSE = \sqrt{\left(\frac{1}{m-2}\right)\sum_{i=1}^{m}\left(q_{i,\exp} - q_{i,cal}\right)^2} \quad ...(2)$$

$$\chi^2 = \sum_{i=1}^{m}\frac{\left(q_{i,\exp} - q_{i,cal}\right)^2}{q_{i,\exp}} \quad ...(3)$$

where $q_{i,exp}$ and $q_{i,cal}$ are obtained from the experiment result and estimation result *via* the adsorption isotherm equation, *m* is the number of observation in the experimental isotherm. A smaller *RMSE* value indicates a better curve fitting, moreover, if the data obtained from the model are close to the experimental results, χ^2 will be a small number[22,28].

RESULTS AND DISCUSSIONS

Synthesis and characterization of material

The effect of the Cd^{2+} ion concentration used as a template on synthesis of Cd(II)-IIP material from the amino-silica hybrid was studied with using the initial concentration for Cd(II)-IIPa, Cd(II)-IIPb, and Cd(II)-IIPc of each 0.05, 0.10, and 0.15 mol L^{-1} resulting the ionic imprinted cavity fraction for each 97.89 (Cd(II)-IIPa), 98.49 (Cd(II)-IIPb), and 95.82 % (Cd(II)-IIPc).

In order to identify the active sites playing a role to the Cd^{2+} ion adsorption, identification of functional groups, surface morphology, element compositions, surface area, volume, and porous diameter of the adsorbent were investigated in this experiment. IR spectra resulted on analysis of adsorbents, Cd(II)-IIPa, Cd(II)-IIPb, and Cd(II)-IIPc, if they were compared with NIP, they do not show difference significantly (Fig. 1). These indicate that the NIP ionic imprinting process to be Cd(II)-IIP does not change the functional group type on Cd(II)-IIP.

From Fig. 1, it can be seen that on Cd(II)-IIP and NIP show relatively similar IR band appearing new band at 2939, 52 cm^{-1} indicating stretching vibration of CH_2 group and at 1640-1560 cm^{-1} indicating bend vibrations of primer amine (N-H) [9,29].

Fig. 2 shows that the surface morphology of Cd-P (Cd with the amino-silica hybrid) (Fig. 2(b)) appears to be brighter than the surface morphology of NIP (Fig. 2(a)) and Cd(II)-IIPb (Fig. 2(c)). This is caused on the Cd-P existed Cd atom producing brighter color (higher accelerating) resulted by Cd atom having high atomic number on the material of Cd-P.

From the surface morphology of NIP, CdP, and Cd(II)-IIPb material (Fig. 2(a-c)) supported by the EDX spectra of NIP (Fig. 2(d)) exists only silica, carbon, nitrogen, and oxygen. But, in Fig. 2(e) for CdP, besides the elements (silica, carbon, nitrogen, and oxygen), Cd is found as a template in the ionic imprinted synthesis. The Cd(II) ions were released to produce the ionic imprinted cavity as seen in the EDX spectra from Cd(II)-IIPb (Fig. 2(f)).

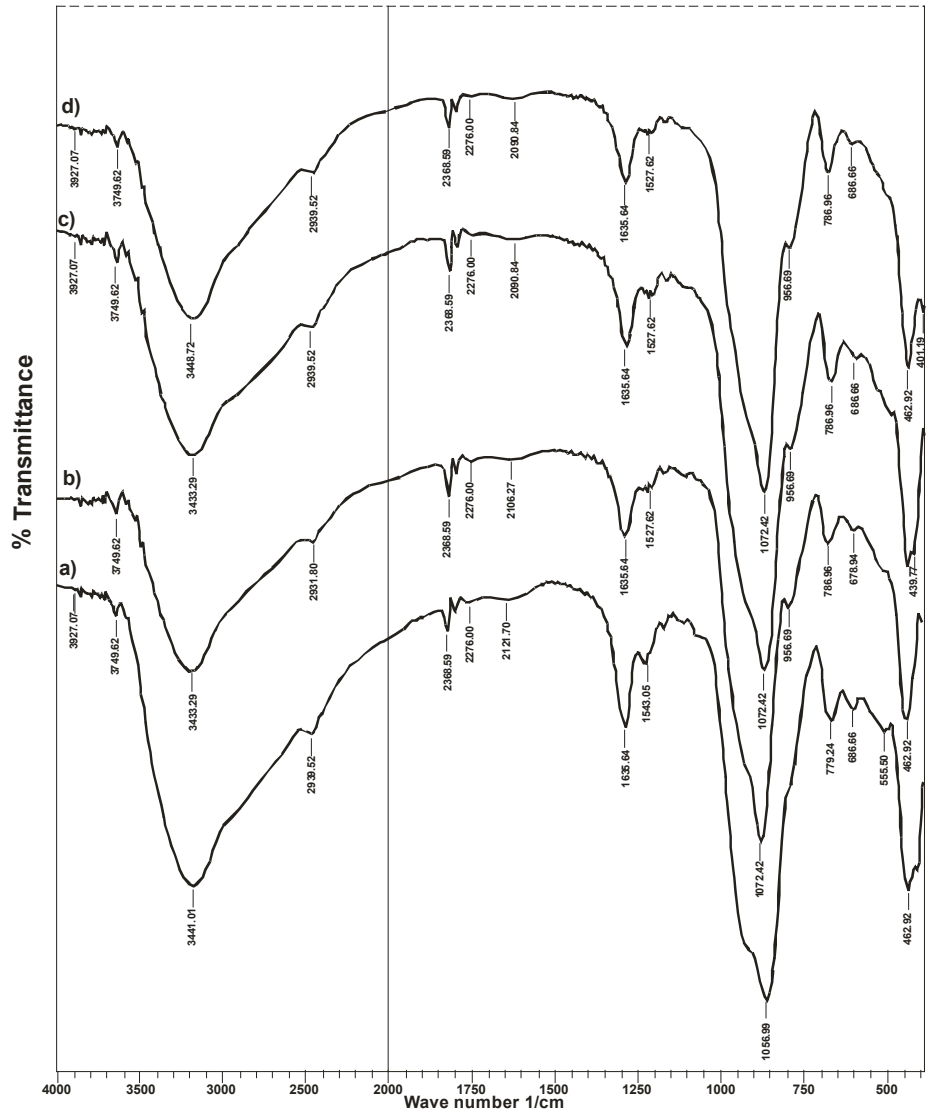

Fig. 1: Infrared spectra of (a) NIP, (b) Cd(II)-IIPa, (c) Cd(II)-IIPb, and (d) Cd(II)-IIPc

In Fig. 3, it can be observed that nitrogen adsorption-desorption isotherm model and graph of relationship between pore volume and pore diameter resulted from measurement of Cd(II)-IIP isotherm tend to follow adsorption isotherm combination of type I and IV based on Brunnauer classification. The adsorption isotherm model of type I occurs in the area of low P/Po, this case can be seen from

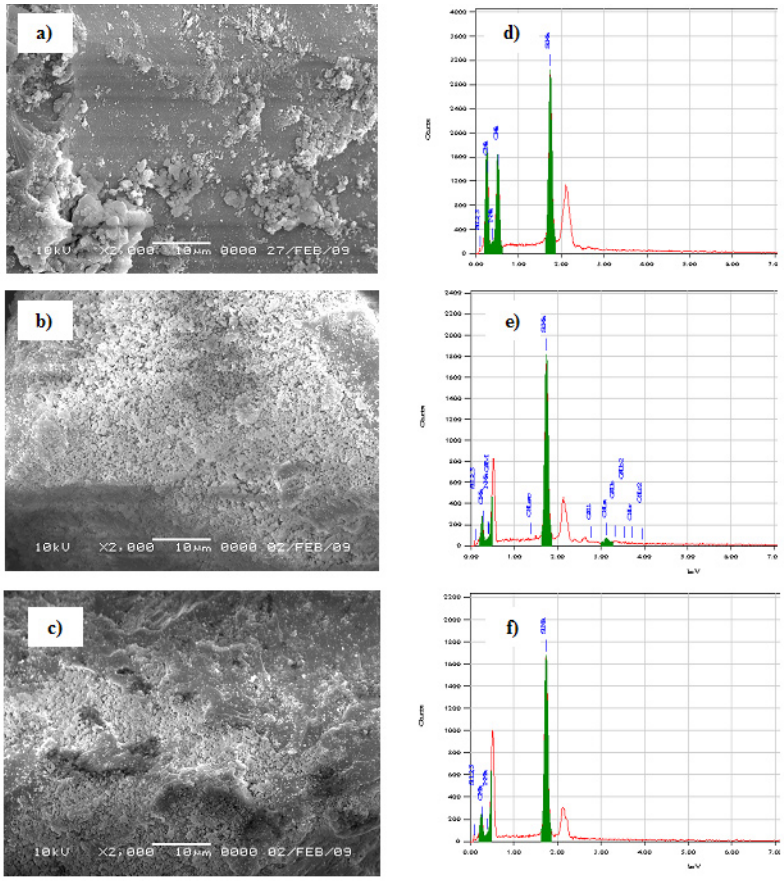

Fig. 2: SEM Images of (a) NIP, (b) Cd-P, and (c) Cd(II)-IIPb as well as EDX spectra of (d) NIP, (e) Cd-P, and (f) Cd(II)-IIPb

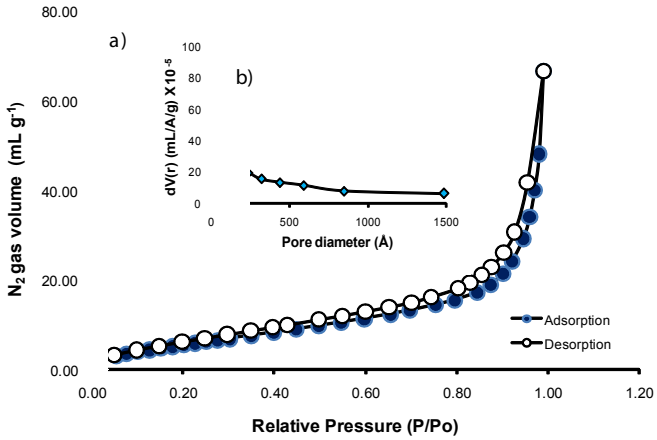

Fig. 3: (a) Nitrogen adsorption-desorption isotherms and (b) pore size distribution of Cd(II)-IIPb

the isotherm form that tends to be horizontal. The isotherm model of type I forms only one layer of adsorbate and it occurs on chemisorption process. While, the isotherm model of type IV occurs in the area of higher P/Po indicated with the adsorption pattern increase that designating adsorption on porous material. This fact is also supported with pore diameter size of 30.45 Å with specific surface area of 29.01 m^2 g^{-1} and total pore volume of 0.29 mL g^{-1}. From the characterization result of the surface characteristic of Cd(II)-IIP material shows that the material is mesoporous. In addition, it can be stated that the active sites of Cd(II)-IIP material are not only determined by active group modification on silica (amino (-NH), silanol (-Si-OH), and siloxane (-Si-O-Si-)), but also determined by the material surface characteristic produced during the ionic imprinting process takes place.

Table 1: Results of plot ln (*m*) vs ln (L_n) on Cd(II)-IIP at the H^+ ion concentrations of 0.5, 1.0, 1.5, 2.5, and 5.0 mmol L^{-1}

H^+ (mmol L^{-1})	0.50	1.00	1.50	2.50	5.00
R^2	0.99	0.97	0.93	0.91	0.96
n	0.48	0.49	0.51	0.49	0.47

Effect of H^+ ion concentration on adsorption process

Adsorption of Cd^{2+} ion on non-imprinted ionic (NIP), Cd(II)-IIPa, Cd(II)-IIPb, and Cd(II)-IIPc in solution media with various concentrations of H^+ ions can be seen in Fig. 4. In Fig. 4, it can be observed that each material of NIP, Cd(II)-IIPa, Cd(II)-IIPb, and Cd(II)-IIPc with the different ionic imprinted fraction shows a similar adsorption model relatively, the higher concentration of H^+ ion the lower amount of Cd^{2+} ion adsorbed (*q*). These facts

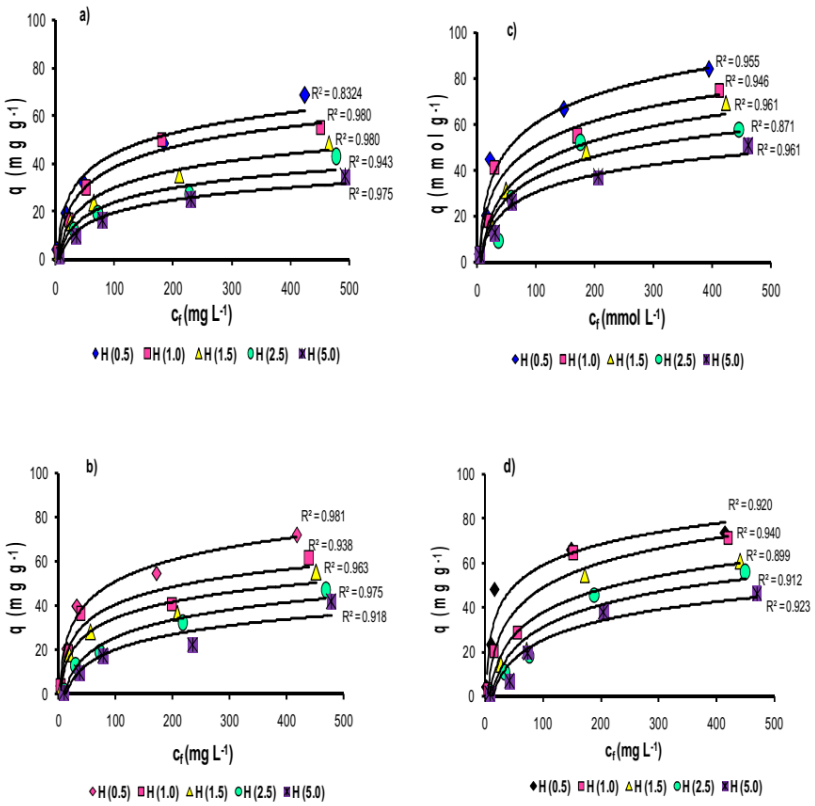

Fig. 4: Adsorption models of Cd^{2+} ions on (a) NIP, (b) Cd(II)-IIPa, (c) Cd(II)-IIPb, and (d) Cd(II)-IIPc with each H^+ ion concentration solution media of 0.5, 1.0, 1.5, 2.5, and 5.0 mmol L^{-1}

indicate that with increasing of H^+ ion, the adsorption ability of the Cd(II)-IIP material from the amino-silica hybrid to Cd^{2+} ion will decrease. In this case, H^+ ion competes with Cd^{2+} ion to place the active sites on the adsorbent.

With using SAS model developed by Su *et al.*[26], adsorption competition of H^+ and Cd^{2+} ions to Cd(II)-IIP material are known according to a theoretical study proposed with an isotherm equilibrium equation of (M^{n+}) metal ion as follows:

$$\frac{Q}{c_f} = K_a\left[\frac{(1+\sigma)L_n - nQ}{1+K_s\cdot c_H^{\alpha}}\right]^n \quad ...(4)$$

For Eq. (4), the Cd^{2+} concentration (C_f) in the dilute solution approaches zero, and therefore Q approaches zero. As a result, the isotherm reduces to

$$\lim_{c_f \to 0}\frac{Q}{c_f} = K_a\left[\frac{L_n}{1+K_s\cdot c_H^{H}}\right]^n$$

Table 2: Comparison between the pseudo-first-order and the pseudo second-order Cd^{2+} ion adsorption kinetic model on NIP, Cd(II)-IIPa, Cd(II)-IIPb, and Cd(II)-IIPc

	Adsorbents			
	NIP	**Cd(II)-IIPa**	**Cd(II)-IIPb**	**Cd(II)-IIPc**
q_e (mg g^{-1})	23.094	20.697	20.253	25.178
Kinetic models				
Pseudo-first-order				
k_1 (min^{-1})	0.041	0.073	0.094	0.028
q_e cal (mg g^{-1})	23.469	20.817	20.291	25.155
R^2	0.992	0.996	0.997	0.991
RMSE	0.025	0.010	0.011	0.015
X^2	0.009	0.001	0.002	0.003
Pseudo-second-order				
k_2 (g mg^{-1} min^{-1})	27.808	84.823	130.114	70.031
q_e cal (mg^{-1} g^{-1})	11.814	16.400	17.757	11.419
R^2	0.749	0.949	0.958	0.876
RMSE	0.289	0.198	0.160	0.280
X^2	0.849	0.440	0.301	0.817

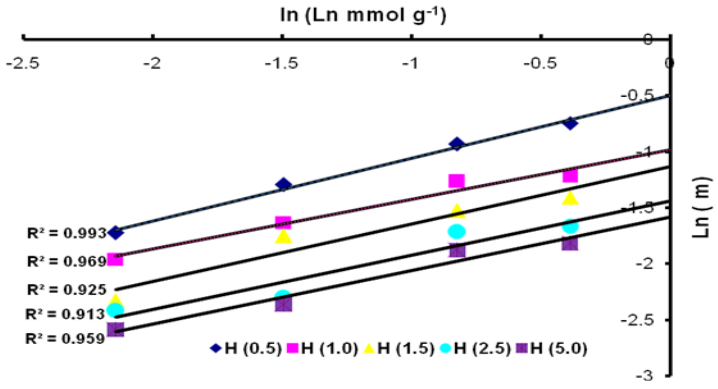

Fig. 5: Plot ln(m) vs ln(L_n) on Cd(II)-IIP material at H^+ ion concentrations of 0.5, 1.0, 1.5, 2.5, and 5.0 mmol L^{-1}

$$(Q \to 0, \sigma \to 0) \quad ...(5)$$

Eq. (5) is used to determine the model parameters K_a, K_s, n, and a. For a dilute Cd^{2+} solution, the partition coefficient, m of Cd^{2+} between adsorbent and solution phases at equilibrium is defined as

$$m = \frac{Q}{c_f} \quad ...(6)$$

In this case, Langmuir isotherm was used as experiment data approach because Langmuir equation can establish the adsorption of metal ion dissolved.

$$Q = \frac{Q_m \cdot c_f}{K_d + c_f} \quad ...(7)$$

when C_f is close to zero, partition coefficient

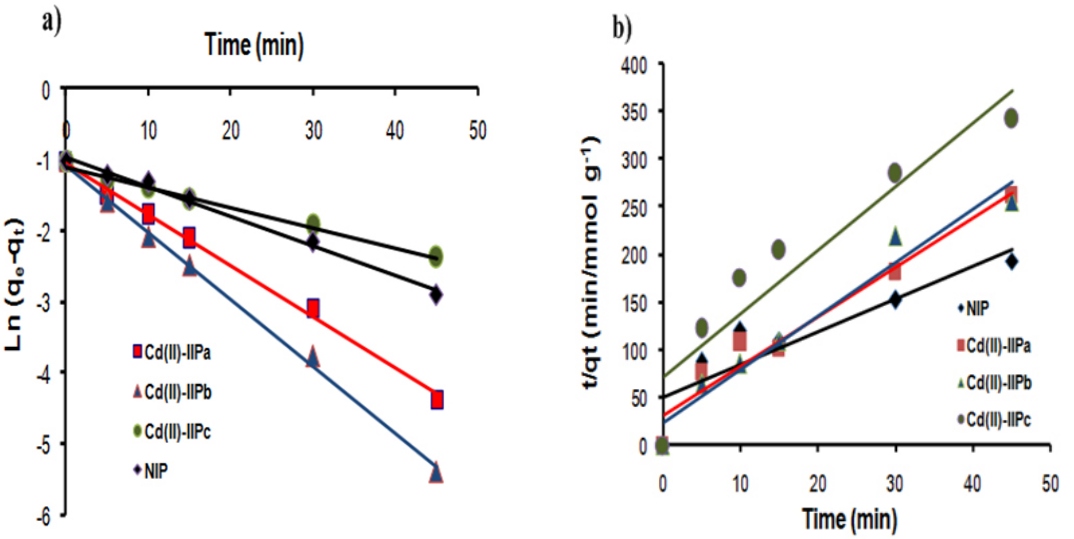

Fig. 6: Kinetic linear models of (a) pseudo first order and (b) pseudo second order on NIP and Cd(II)-IIP at 27 °C, pH of 6, Cd(II) concentration of 100 mg L^{-1}, volume of 20 mL, and adsorbent mass of 50 mg

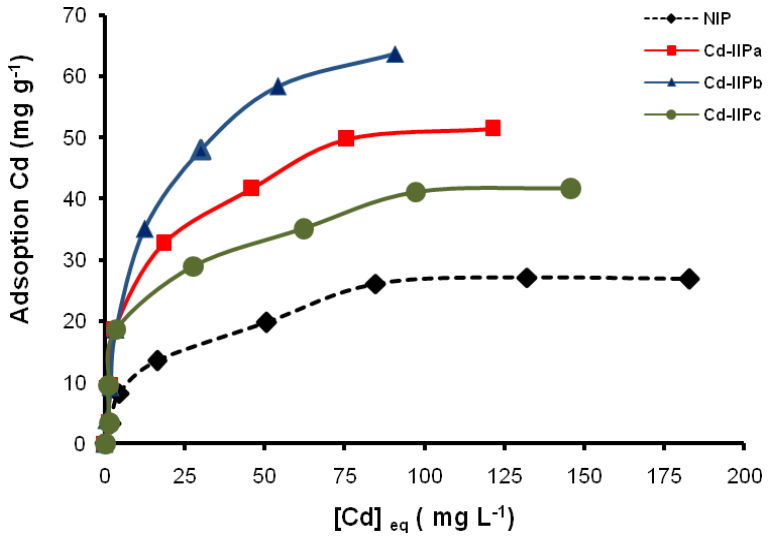

Fig. 7: Curves of relationship between the Cd^{2+} ion equilibrium concentration and the amount of Cd^{2+} ion adsorbed at temperature of 27 °C, pH of 6, time of 60 min, volume of 20 mL, and adsorbent mass of 50 mg

m from Cd^{2+} will be the same with the slope from the adsorption isotherm, namely:

$$m = \frac{Q}{c_f} = \frac{Q_m}{K_d} \quad (c_f \to 0)$$

...(8)

Thus, the partition coefficient can be estimated from the Eq. (8).

Substituting Eq. (8) into Eq. (5) and rearranging yields the following equation:

$$m = \frac{Q}{c_f} = K_a \left[\frac{L_n}{1 + K_s \cdot c_H^{\alpha}} \right]^n$$

...(9)

Assuming that the linear model parameters, K_a, K_S, *n* and *a* are independent of the surface active site concentration on the adsorbent surface, the values of these parameters can be obtained by taking the logarithm of both sides of Eq. (9)

$$\ln m = n \ln L_n + \ln K_a - n \ln\left[1 + K_s \cdot c_H^{\alpha}\right]$$

...(10)

This plot of ln(*m*) versus ln(L_n) should yield a straight line with the following properties:

Slope = *n* ...(11)

Table 3: Adsorption parameters of Cd^{2+} ions on NIP and Cd(II)-IIP with Langmuir, Freundlich, Dubinin-Raduskevich, and Temkin Equations (pH of 6 and temperature of 27 °C)

	Adsorbents			
	NIP	**Cd(II)-IIPa**	**Cd(II)-IIPb**	**Cd(II)-IIPc**
Adsorption isotherms				
Langmuir				
q_m (mg g^{-1})	28.823	54.304	62.105	43.402
K_L x 10^3 (L mol^{-1})	8.644	13.076	15.863	14.254
R^2	0.990	0.990	0.991	0.990
RMSE	2.311	3.478	3.266	4.377
$\chi 2$	1.683	3.427	2.412	7.327
Freundlich				
K_f (mg g^{-1})	3.270	6.445	7.138	6.831
n	2.263	2.072	1.955	2.527
R^2	0.930	0.874	0.935	0.794
RMSE	3.283	7.836	10.093	5.463
$\chi 2$	2.944	10.778	11.765	10.724
Dubinin-Raduskevich				
q_{DR} (mg g^{-1})	26.396	54.315	59.472	41.157
B_{DR} x 10^{-3} (mol^2 kJ^{-2})	2.104	1.815	1.659	1.495
R^2	0.976	0.953	0.992	0.827
RMSE	2.302	3.563	3.332	3.985
$\chi 2$	1.466	3.183	1.281	7.559
Temkin				
b_{Te} (J mol^{-1})	2.206	3.987	4.496	2.884
a_{Te} (L g^{-1})	1.023	1.086	1.114	1.048
R^2	0.975	0.993	0.972	0.963
RMSE	1.691	1.822	4.058	3.232
$\chi 2$	7.170	1.138	7.170	9.242

$$Intercept = \ln K_a - n \ln\left[1 + K_s \cdot c_H^{\alpha}\right] \quad ...(12)$$

where, C_H is the concentration of H^+ ions in solution (mmol L^{-1}), *a* is an amount of H^+ binding site characteristic, C_f is the concentration of Cd^{2+} ion in solution (mmol L^{-1}), C_i is the initial concentration of Cd^{2+} ion in solution (mmol L^{-1}), K_a is the equilibrium constants of Cd^{2+}, K_d is the dissociation constants of Langmuir equation (mmol L^{-1}), K_s is the equilibrium constants of H^+, L_a is the concentration of adsorption active site that is not occupied (empty) on adsorbent surface (mmol g^{-1} adsorbent), L_n is the total amount of the concentration of active site ionic imprinted on adsorbent surface that is the amount of concentration Cd^{2+} ion used in ionic imprinting process (mmol g^{-1} adsorbent), *m* is the partition coefficient between Cd^{2+} ion and solution, *n* is the amount of binding site characteristic for Cd^{2+}, *Q* is the concentration of Cd^{2+} adsorbed by adsorbent (mmol g^{-1} adsorbent), Q_m is the adsorption capacity in Langmuir adsorption isotherm equation (mmol g^{-1} adsorbent), *ó* is non-imprinted factor[26].

If the data of Fig. 4 were plotted using Eq. 10, then it can be produced Fig. 5 showing the relationship between L_n and *m* to determine the value of *n* displayed in Table 1. From Fig. 5, it can be observed that generally plot of logarithm from partition coefficient resulted from the Langmuir adsorption isotherm equation, ln(*m*) versus ln(L_n) produced straight line for each concentration variation of H^+ with the slope *n* that is nearly similar of 0.5 which means that one active site binds to two Cd^{2+}ions.

Adsorption kinetics

In order to know Cd^{2+} ion adsorption kinetic model on NIP and Cd(II)-IIP, adsorption data were evaluated with using pseudo-first-order (Eq. (13)) and pseudo-second-order (Eq. (14)) kinetic model as follow[23,30]:

$$q_t = q_e\left(1 - e^{-k_1 t}\right) \quad ...(13)$$

$$q_t = \frac{q_e^2 k_2 t}{1 + q_e k_2 t} \quad ...(14)$$

where q_t and q_e (mg g^{-1}) are total Cd^{2+} ions adsorption capacity at time *t* and at equilibrium, respectively, k_1 and k_2 are the first order and second order rate constants, respectively.

Analysis results of kinetic models are displayed in Fig. 6(a) for the pseudo-first-order kinetic model and Fig. 6(b) for the pseudo second-order kinetic model. Table 2 shows total Cd^{2+} ions adsorption rate constants (k_1 and k_2) and correlation coefficients calculated using linearized plots of Eqs. (13) and (14), respectively. In addition, *RMSE* and χ^2 (Eqs. (2) and (3)) were determined to know Cd^{2+} ions adsorption kinetic model tendency on NIP and Cd(II)-IIP with the different ionic imprinted cavity fractions.

In Table 2 can be seen that Cd^{2+} ion adsorption process on NIP and Cd(II)-IIP tends to follow the pseudo-first-order kinetic model stated with average linear regression coefficient value (R^2) 0.99. This tendency is also supported by *RMSE* and χ^2 smaller than the pseudo second-order kinetic model showing that the data obtained from estimation result using the pseudo first-order kinetic model having value closing with the experiment results. In generally, in Table 2 was observed that k_1 of Cd^{2+} ion on the Cd(II)-IIPb adsorbent was relatively higher than the Cd(II)-IIPa and the Cd(II)-IIPc.

Adsorption isotherm

The effect of initial concentration of Cd^{2+} ion solution on NIP and Cd(II)-IIP to investigate tendency of the adsorption isotherm model can be seen in Fig. 7. Fig. 7 displays the Cd^{2+} ion adsorption isotherm model on NIP and Cd(II)-IIP with initial various concentrations showing that the Cd^{2+} ion adsorption increased constantly with increasing of metal ion concentration and at relatively higher concentration, increasing of metal ion concentration did not anymore followed with increasing of Cd^{2+} ion adsorption on the adsorbent significantly. The adsorption isotherm models applied to evaluate adsorption process running were Langmuir (Eq. (15)), Freundlich (Eq. (16)), Dubinin-Raduskevich (Eqs. (17) and (18)), as well as Temkin (Eq. (19)) adsorption isotherm[31,32].

$$q_e = q_m \frac{K_L C_e}{1 + K_L C_e} \quad ...(15)$$

$$\log q_e = \log K_f + \frac{1}{n} \log C_e \quad ...(16)$$

$$q_e = q_{DR} \exp(-B_{DR}\varepsilon_{DR}^{\ 2}) \quad ...(17)$$

$$\varepsilon_{DR} = RT(1+\frac{1}{C_e}) \quad ...(18)$$

$$q_e = \frac{RT}{b_{Te}} \ln(K_{Te}C_e) \quad ...(19)$$

where, q_m is the maximum metal ion amount adsorbed (mg g^{-1}), C_e is the metal ion equilibrium concentration (mL g^{-1}), n is the Freundlich exponent, K_L (L mol^{-1}) and K_F (mg g^{-1}) is each the Langmuir and Freundlich constant. The ε_{DR}, the Polanyi potential, is a constant related to the adsorption energy, q_{DR} and B_{DR} are the *D-R* isotherm constants in mg g^{-1} and mol^2 kJ^{-2} respectively, b_{Te} is the Temkin constant related to the heat adsorption (J mol^{-1}), K_{Te} is the equilibrium binding constant L g^{-1}, R is the gas constant (8.314 kJ mol^{-1}), and T is the absolute temperature (K).

Parameters of Cd^{2+} ion adsorption isotherm on NIP and Cd(II)-IIP from isotherm equations of Langmuir, Freundlich, Dubinin-Radushkevich, and Temkin (Table 3) show that generally, Cd^{2+} ion adsorption data follow adsorption isotherm model of Langmuir with average of R^2 around 0.99 supported by lower *RMSE* and $\chi 2$. These facts give an indication that Cd^{2+} ion adsorption on NIP and Cd(II)-IIP characterized as monolayer.

In Table 3, it can be seen that increasing of adsorption capacity occurred on Cd(II)-IIP higher than NIP. Surface of Cd(II)-IIP material was to be more selective and specific upon metal ion used as a template. The existence of appropriate acid and base character between Cd^{2+} ion and N atom as donor in complex formation in synthesis of ionic imprinted material will produce a selective material to the target metal because the interaction of metal ions and the material runs to be stronger and also to be more selective.

Adsorption capacity of Cd^{2+} ion on Cd(II)-IIPb material is relatively bigger than Cd(II)-IIPa and Cd(II)-IIPc material (Table 3), these results are accordance with the results obtained on determination of the adsorption kinetic model pseudo second order. Evaluation result of the adsorption isotherm shows that difference of template metal ion concentrations (ionic imprinted cavity fraction) will give effect on the metal ion adsorption isotherm model adsorbed.

If the data of Cd^{2+} ion adsorption capacity on the Cd(II)-IIP material (Table 3) were compared with other research results about the Cd^{2+} ionic imprinted material as the material of dual-ligand reagent (2Z)-N,N'-bis(2-aminoethylic)but-2-enediamide-Cd^{2+} with the batch method adsorption resulting adsorption capacity of 32.56 mg g^{-1} [33]. Adsorption of Cd^{2+} ion with the continue method using phenol-formaldehydeCd(II)-2- (p-sulphophenylazo-1,8-dehyroxynapthalene,3,6-disulphonate and polymer Cd(II)-2,2-{thane-1,2-diylbis[nitrilo (E) methyl]}lidene diphenolate-4-vinyl pyridine produced the adsorption capacity of 0.27 and 0.48 mg g^{-1}, respectively[34,35]. From the research result, it can be known that the adsorption capacity of Cd^{2+} ion on Cd(II)-IIP is relatively the highest among the other materials in adsorbing the target metal ion.

CONCLUSIONS

From the evaluation results of the adsorption kinetic and adsorption isotherm parameters show that the values of the adsorption rate and capacity of ionic imprinted materials on Cd(II)-IIPa, Cd(II)-IIPb, Cd(II)-IIPc are bigger than NIP. The Cd^{2+} ionic imprinting cavity fraction played a role as active sites prepared from different concentrations of Cd^{2+} ion produces different adsorption rate and capacity with ion target (Cd^{2+} ion). Adsorption competition of Cd^{2+} and H^+ ion to active sites is influential to number of Cd^{2+} ion adsorbed on NIP and Cd(II)-IIP. The higher the concentration of H^+ ions, the lower the number of Cd^{2+} ions adsorbed. The Cd^{2+} ionic imprinted material from amino-silica hybrid can be used as effective material to bind Cd^{2+} ions in solution.

ACKNOWLEDGEMENTS

The authors would like to thank the Directorate of Research and Community Services, Directorate General of Higher Education (DIKTI), Ministry of Research, Technology and

Higher Education of the Republic of Indonesia (Kemenristekdikti) for funding this research through Fundamental Research Grant with contract number: 040/SP2H/LT/DRPM/II/2016.

REFERENCES

1. Hajiaghababaei, L.; Badiei, A.; Ganjali, M.R.; Heydari, S.; Khaniani, Y.; Ziarani, G.M. *Desalination*. **2011**, *266*, 182-187.
2. Suharso; Buhani. *Asian J. Chem.* **2011,** *23(3),* 1112-1116.
3. Buhani; Suharso; Sembiring, Z. *Orient. J. Chem*. 2012, *28(1)*, 271-278.
4. Newton, D.E. *Chemistry of the Environment*, Fact on File, an Imprint of Infobase Publishing, New York, **2007**.
5. National Library of medicine, *Hazardous Substance Data Bank (HSDB)*, **1996**.
6. Buhani; Suharso; Fitriyani, A.Y. *Asian J. Chem.* **2013,** *25(5)*, 2875-2880.
7. Buhani; Suharso; Sumadi. *Asian J. Chem.* **2012**, *24(1)*, 133-140.
8. Buhani; Suharso. *Asian J. Chem.* **2009**, *21(5)*, 3799-3808.
9. Buhani; Narsito; Nuryono; Kunarti, E.S.; Suharso. *Desalin. Water Treat*. **2015**, *55*, 1240-1252.
10. Buhani; Suharso; Aprilia, L. *Indo. J. Chem*. **2012**, *12(1)*, 94-99.
11. Alcantara, E.F.C.; Faria, E.A.; Rodrigues, D.V.; Evangelista, S.M.; DeOliveira, E.; Zara, L.F.; Rabelo, D.; Prado, A.G.S. *J. Colloid Interf. Sci.* **2007**, *311*, 1-7.
12. Cui, Y.; Chang, X.; Zhu, X.; Luo, H.; Hu, Z.; Zou, X.; He, Q. *Microchem. J.* **2007,** *8*, 20-26.
13. Chang, X.; Wang, X.; Jiang, N.; He, Q.; Zhai, Y.; Zhu, X.; Hu, Z.; *Microchim. Acta*. **2008**, *162*, 113-119.
14. He, Q.; Chang, X.; Zheng, H.; Jiang, N.; Wang, X.; *Intern. J. Environ. Anal. Chem.* **2008**, *88(6)*, 373-384.
15. Zhang, N.; Suleiman, J.B.; He, M.; Hu, B. *Talanta*. **2008**, *75*, 536-543.
16. Chen, N.; Zhang, Z.; Feng, C.; Li, M.; Zhu, D.; Sugiura, N. *Mater. Chem. Phys.* **2011**, *125*, 293-298.
17. Liu, H.; Yang, F.; Zheng, Y.; Kang, J.; Qu, J.; Chen, P. *Water Res*. **2011**, *45*, 145-154.
18. Arbab-Zavar, M.H.; Chamsaz, M.; Zohuri, G.; Darroudi, A. *J. Hazard. Mater.* **2011**, 185, 38-43.
19. Li, F.; Jiang, H.; Zhang, S. *Talanta*. **2007**, *71*, 1487-1493.
20. Zhao, J.; Han, B.; Zhang, Y.; Wang, D. *Anal. Chim. Acta*. **2007**, *603*, 87-92.
21. Zhai, Y.; Liu, Y.; Chang, X.; Ruan, X.; Liu, J. *React. & Funct. Polymers*. **2008**, *68*, 284-291.
22. Montazer-Rahmati, M.M.; Rabbani, P.; Abdolali, A.; Keshtkar, A.R.; *J. Hazard. Mater.* **2011**, *185*, 401-407.
23. Bermúdez, Y.G.; Rico, I.L.R.; Bermúdez, O.G.; Guibal, E. *Chem. Eng. J*. **2011**, *166*, 122-131.
24. Zakhama, S.; Dhaouadi, H.; M'Henni, F.; *Biores. Technol*. **2011**, *102*, 786-796.
25. Ho, Y.S.; Porter, J.F.; McKay, G. *Water Air Soil Pollut*. **2002**, *141*, 1-33.
26. Su, H.; Chen, S.; Tan, T. *Process Biochem.* **2007**, *42*, 612-619.
27. Buhani; Narsito; Nuryono; Kunarti, E.S. *Desalination*. **2010**, *251*, 83-89.
28. Vijayaraghavan, K.; Padmesh, T.V.N.; Palanivelu, K.; Velan, M. *J. Hazard. Mater*. **2006**, *B 133*, 304-308.
29. Machado, R.S.A.; da Fonseca, M.G.; Arakaki, L.N.H.; Espinola, J.G.P.; Oliveira, S.F. *Talanta*. **2004**, *63*, 317-322.
30. Patel, R.; Suresh, S. *Biores. Technol*. **2008**, *99*, 51-58.
31. Ho, Y.S.; Porter, J.F.; McKay, G. *Water Air Soil Pollut*. **2002**, *141*, 1-33.
32. Periæ, J.; Trgo, M.; Medvidoviæ, N.V. *Water Res*. **2004**, *38*, 1893-1899.
33. Zhai, Y.; Liu, Y.; Chang, X.; Chen, S.; Huang, X. *Anal. Chim. Acta*. **2007**, *593*, 123-128.
34. Candan, N.; Tüzmen, N.; Andac, M.; Andac, C.A.; Say, R.; Denizli, A. *Mater. Sci. Eng.* **2009**, *C 29*, 144-152.
35. Gawin, M.; Konefal, J.; Trzewik, B.; Walas, S.; Tobiasz, A.; Mrowiec, H.; Witek, E. *Talanta*. **2010**, 80, 1305-1310.